

The definitive version is available at <http://www.interscience.wiley.com/>.

F.P. Vidal, N.W. John, D.A. Gould, and A.E. Healey: Simulation of Ultrasound Guided Needle Puncture using Patient Specific Data with 3D Textures and Volume Haptics. *Computer Animation and Virtual Worlds* (May 2008), John Wiley & Sons. Volume 19, Issue 2, pp. 111-127.

DOI: 10.1002/cav.217

**Keywords:** medical virtual environment; imaging guidance; interventional radiology training; needle puncture; volume haptics; vertex and pixel shaders.

```
@ARTICLE{Vidal2008ComputAnimatVirtW,
  author = {F. P. Vidal and N. W. John and D. A. Gould and A. E. Healey},
  title = {Simulation of Ultrasound Guided Needle Puncture using Patient Specific
Data with {3D} Textures and Volume Haptics},
  journal = {Computer Animation and Virtual Worlds},
  year = {2008},
  volume = {19},
  pages = {111-127},
  number = {2},
  month = May,
  abstract = {We present an integrated system for training ultrasound (US) guided
needle puncture. Our aim is to provide a validated training tool
for interventional radiology (IR) that uses actual patient data.
IR procedures are highly reliant on the sense of touch and so haptic
hardware is an important part of our solution. A hybrid surface/volume
haptic rendering of an US transducer is proposed to constrain the
device to remain outside the bony structures when scanning the patient's
skin. A volume haptic model is proposed that implements an effective
model of needle puncture. Force measurements have been made on real
tissue and the resulting data is incorporated into the model. The
other input data required is a computed tomography (CT) scan of the
patient that is used to create the patient specific models. It is
also the data source for a novel simulation of a virtual US scanner,
which is used to guide the needle to the correct location.},
  doi = {10.1002/cav.217},
  keywords = {medical virtual environment; imaging guidance; interventional radiology
training; needle puncture; volume haptics; vertex and pixel shaders},
  publisher = {John Wiley \& Sons}
}
```

# Simulation of Ultrasound Guided Needle Puncture using Patient Specific Data with 3D Textures and Volume Haptics

F. P. VIDAL<sup>1</sup>, N. W. JOHN<sup>1</sup>, D. A. GOULD<sup>2</sup>, and A. E. HEALEY<sup>3</sup>

<sup>1</sup> School of Computer Science, University of Wales, Bangor, UK,

<sup>2</sup> Royal Liverpool University and Broadgreen Hospitals NHS Trust, UK,

<sup>3</sup> Royal Liverpool Childrens Hospital Alder Hey NHS Trust,  
Royal Liverpool University and Broadgreen Hospitals NHS Trust, UK

## Abstract

We present an integrated system for training ultrasound (US) guided needle puncture. Our aim is to provide a validated training tool for interventional radiology (IR) that uses actual patient data. IR procedures are highly reliant on the sense of touch and so haptic hardware is an important part of our solution. A hybrid surface/volume haptic rendering of an US transducer is proposed to constrain the device to remain outside the bony structures when scanning the patient's skin. A volume haptic model is proposed that implements an effective model of needle puncture. Force measurements have been made on real tissue and the resulting data is incorporated into the model. The other input data required is a computed tomography (CT) scan of the patient that is used to create the patient specific models. It is also the data source for a novel simulation of a virtual US scanner, which is used to guide the needle to the correct location.

**Keywords:** medical virtual environment; imaging guidance; interventional radiology training; needle puncture; volume haptics; vertex and pixel shaders.

## 1 Introduction

The practice of interventional radiology (IR) uses imaging to guide catheters (tubes) and wires through organ systems using a small portal of entry (minimal access) into the body. As a result, IR techniques generally have less risk, less postoperative pain and shorter recovery time compared to open surgery. IR extends to a vast range of imaging guided procedures which are minimally invasive. Targeted treatments are performed using imaging for guidance in all organ systems, including the liver, the urinary tract, biliary system, gut and blood vessels in the field of many different medical and surgical specialities [23]. These procedures include angioplasty, embolisation, thrombectomy, biopsy, nephrostomy, percutaneous biliary access, aneurysm endograft, vertebroplasty, gastrostomy, radiofrequency tumour ablation. Fluoroscopic imaging, computed tomography (CT), ultrasound (US), or other imaging modalities are used for guidance. US is particularly commonly used for biopsy [33, 22] and nephrostomy [25]. More recently, real-time magnetic resonance imaging (MRI) has also been used for IR guidance [4].

At the same time, there is a growing need for alternatives to the traditional medical apprenticeship training model currently used in IR. Apprenticeship training methods where procedures are learnt and skills obtained during practice in patients is becoming less desirable due to several factors. These factors include: regulatory restrictions on working hours during training years; replacement of invasive diagnostic procedures (the traditional IR training arena) by non-invasive CT and MR imaging methods; patient discomfort, pain and complications resulting from an inexperienced trainee; de-skilling of rarely performed procedures; variability of a trainee's exposure to

case mix and emergency work; and expansion of traditional IR procedures into other disciplines. An alternative to training in patients is therefore urgently needed.

The potential for the use of computer graphics in medicine has been well established, and applications include diagnostic tools, intra-operative planning aids, education tools, and training simulators. A full survey of the current state-of-the-art can be found in [34]. An important emerging area is the provision of training tools for IR procedures. In using some form of simulation to replace patients, computer based simulations of guidewire and catheter insertion for IR are already available commercially, and the best examples are discussed in the section on ‘Related work’. However, training of needle puncture guided by imaging (e.g. ultrasound, computed tomography or any other imaging modality) using the Seldinger technique - the first step in approximately half of all IR procedures - has been largely overlooked.

Our aim is to address this deficiency by providing a cost effective, configurable and validated training tool to enable IR practitioners to learn how to carry out image guided needle puncture.

Early results using a single haptic device are presented in [35]. In this version the user could not use the virtual probe and virtual needle simultaneously, and no hardware acceleration was used for computing CT or X-Ray images. Our new research contributions presented here are to use actual patient data to mimic the same visual and haptic sensation as found with a real patient using two haptic devices - including a hybrid surface/volume haptic rendering of an ultrasound transducer, a fast and accurate needle force model, and a novel solution for simulating real time ultrasound images using hardware acceleration when possible.

The section on ‘Materials and Methods’ begins by describing the hardware components that have been used to build the system (see the subsection on ‘System description’). While visual cues are needed for accurate targeting, a high fidelity haptic interface is also particularly important in simulating IR procedures as the sense of touch and force feedback are key to avoid damage or complications in patients. Our volume haptic models are then described in detail (see the subsection on ‘Haptic rendering’).

The input data required is an anatomical CT scan specific to a particular patient’s anatomy and pathology, although for ethical and Research Governance requirements, the identity of any patient is withheld and all imaging data is anonymised. These data are then used to create the patient specific anatomical models, which can be viewed in stereo if required (see the subsection on ‘Data acquisition and visualization’). The CT scan is also used as the source data by our new algorithm to simulate the image output from a virtual ultrasound scanner. Full advantage is taken of texture hardware on modern PC graphics cards for interactive rendering of the 3D models, and programming with framebuffer objects (FBOs), vertex and pixel shaders where appropriate (see the subsection on ‘Reconstructed image rendering’).

The project is a multi disciplinary collaboration involving practising interventional radiologists and computer scientists, and clinical validation of the system’s content has been carried out at each development stage. Results are presented in the penultimate section, and we end the paper with conclusions and a discussion of future work. The paper provides a detailed overview of all of the stages involved in building an integrated medical simulator, and will be of relevance to computer scientists, medical educators, and clinicians in interventional radiology and a range of other disciplines.

## 2 Related work

According to Otto, ultrasound-guided fine-needle abdominal biopsy was first described in 1972 [24]. Matalon and Silver reviewed the use of ultrasound images as a guidance of interventional procedures in the early 90s, and discussed the advantages of US guidance over CT guidance [22]. Finally, they explain how to place a needle into a target under US guidance using the freehand technique. More recently, Chapman *et al* present the basics of ultrasound guided puncture, emphasising how to visualise the needle, and particularly directed at anaesthetists and intensivists [5]. To identify, describe and detail the whole process of core interventional radiology procedures, from the cues perceived, to the cognitive thought processes of decision-making, to the ensuing physical actions,

cognitive task analysis (CTA) studies have been performed by our psychologist partners of the “Collaborators in Radiological Interventional Virtual Environments” (CRaIVE) consortium [7, 18]. This work includes CTA for freehand ultrasound guided biopsy [17], and has been used extensively to guide the design of the simulator described in this paper. An excerpt from this detailed task analysis is included in Table 1. Generally, an important concept of ultrasound-guided procedures

---



---

**Steps of the task:**

1. Place probe on patient at incision site
  2. Looking at the ultrasound screen roll the probe back and forth on the incision site until the planned biopsy site is identified
  3. Note the depth of the planned biopsy site using the markers on the ultrasound screen
  4. Pick up the biopsy trocar (with needle) from the green sheet - make note of the measurement markers on the trocar to identify how deep this needle is going to be inserted
  5. Holding the needle shaft position the biopsy trocar at the incision site
  6. Holding the shaft begin to insert the trocar perpendicular to the skin into incision
  7. Position the trocar, probe and planned biopsy site in the same plane (to ensure all necessary information can be viewed on the ultrasound screen)
  8. Looking at the ultrasound screen jiggle the trocar gently and identify the trocar on the image (a moving needle is easier to identify than a static needle) and the planned biopsy site (the aim is to be able to see both the trocar and the planned biopsy site in the same image)
  9. Slowly advance the trocar towards the planned biopsy site, constantly viewing the ultrasound image to guide orientation and progress
  10. Continue advancing the trocar in this way until the planned biopsy site is reached (the needle should be positioned just short of the planned sample site, if a tumour is being biopsied the needle needs to be at the edge of the tumour), be guided both by the image and by your knowledge of the depth of the planned biopsy site
  11. Request patient to hold their breath
  12. Whilst patient holding their breath check (on the ultrasound screen) positioning of trocar is correct. Is the trocar in the correct position for biopsy?
    - Yes – go to next step (allow patient to breath, shallowly)
    - No – repeat from step 7 (if necessary withdraw the trocar slightly before proceeding) (allow patient to breath)
- 
- 

**Table 1:** Excerpt from [17] related to Ultrasound guided needle puncture using a coaxial biopsy needle. The detailed description of each step of the task has been essential information for designing the simulator described in this paper.

is real-time interaction. To ensure the correct placement of the needle into the target, the practitioner must establish an interactive feedback loop between the real-time US images and the needle placement (see Figure 1). However, US guided techniques have been reported as being underused because of the lack of understanding of real-time ultrasound images, in particular to locate the position of the needle tip [22, 5].

Contrary to open surgery, the practitioner does not look at his/her hands but at a monitor where images are displayed, and for training of the skills required, some hospitals have adopted ‘low tech’ but hi-fidelity home grown solutions. The Manchester Royal Infirmary, for example, makes use of a phantom model built from a plastic box filled with foam into which tube like structures have been hollowed out in order to represent blood vessels. Water is added to the box, which is then placed into a microwave oven for several minutes to remove all of the air bubbles. Figure 2 is another example of home-made mannequin used to teach IR students how to perform ultrasound guided puncture. It consists of a plastic box filled with agar. Olives and grapes are

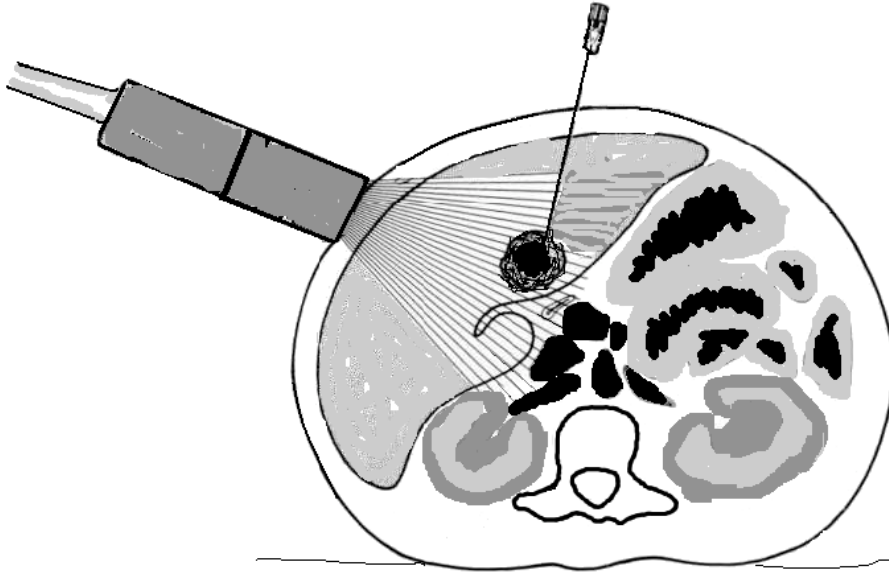


**Figure 1:** Placement of the needle using the freehand technique.



**Figure 2:** On the left-hand side: Home-made mannequin for ultrasound guided needle puncture in use during an annual Interventional study day at the Royal Preston Hospital. On the right-hand side: Example ultrasound image produced.

hidden in the box below the agar, they correspond to targets for the puncture. Finally, water is added to the box. Both of these phantom models can then be used with a conventional ultrasound scanner, and produces images similar in appearance to the ultrasound images of patients that the clinician will see in practice (see Figure 2).

Other proprietary models use tissue mimics to provide effective simulation of ultrasound needle guidance, such as synthetic soft tissue models [20]. Zhu *et al* extend the use of a mannequin further [38]. They use a pair of calibrated magnetic 3D motion sensors to capture the position and orientation of a mock ultrasound probe and needle, whilst emulated ultrasound images are generated in real-time from a labelled volumetric data set that is non-rigidly aligned to the mannequin. Such an approach is relatively affordable, though at the same time the learning process requires a complete range of anatomical and pathological encounters. There are difficulties providing sufficient variety using solutions based on fixed anatomical models, and in addition the tactile properties and physiological responses of foam and other surrogate materials are far from that of a real person. Animal models are expensive and currently they are morally difficult to justify.

Computer based simulation can potentially overcome some of the limitations of fixed models. The first generation of medical training simulators focused on laparoscopic surgery, which is well

suited for computer simulation. More recently products have been introduced aimed at the IR domain such as the Mentice Procedicus VIST system for carotid and renal stenting; the Symbionix Mentor range including training for percutaneous access procedures with real-time fluoroscopy; and Immersion Medical’s AccuTouch Endovascular simulator, which includes support for percutaneous transluminal coronary angioplasty and stent. Often these commercial products have resulted from pioneering work carried out in academia; VIST for example has used the Interventional Cardiology Training System (ICTS) developed by the CIMIT Simulation Group [8]. These systems do not simulate the whole procedure, and few support needle puncture. They also tend to use predefined patient models, and do not yet provide the same fidelity of experience as training on a real person. Successful validation of IR simulators, for training and assessment in IR curricula, remains to be achieved [13].

For image guided needle puncture, the Haptic Operative Realistic Ultrasonography Simulator (HORUS) is the only other computer based simulator to address this problem [11], and is particularly aimed at ultrasound guided needle insertion for biopsy and radio frequency thermal ablation. Two force feedback devices are used by HORUS: one for the ultrasound probe and one for the needle. The algorithm for simulating ultrasound images appears to be based on ray casting, but the implementation details have not been published. The mannequin solution developed at the University of Leeds [38] constructs a set of volumetric textures to represent the typical appearance of ultrasound images, and an alpha blending method is applied to produce a radial blurring effect. Our solution provides an alternative novel method of simulating ultrasound using the Graphics Processing Unit (GPU). It also supports stereoscopic viewing, and different rendering schemes can be used to represent the real-time images displayed to the trainee. Our use of anonymised, real, patient specific imaging data also allows the training simulation to take place on different anatomical regions, using accurate and variable anatomical representation, and with a range of pathological entities. This variability is important to learning.

The use of haptics is a vital component when manipulating virtual tools. Typically, the haptic model implemented is iteratively refined until it reaches a point when a domain expert is satisfied that the kinesthetic sensation is good enough to mimic reality. Look Up Tables (LUTs) containing a sequence of empirically defined values is one approach that has been applied to needle insertion [12]. Each entry in the LUT contains the force value that is applied once the needle has reached a particular depth. Physically-based models that take into account the elastostatic properties of tissues under distortion have also been reported [9]. Other recent work has focused on the measurement of forces during procedural instrumentation of real patients [10, 14]. The data can be used to create and validate a haptic model. In the Hermes project [29] a custom haptic interface for angioplasty has been built using such force measurement data in its design. The user experiences both forces and torque at their fingertips whilst manipulating a catheter like device. Mentice/Xitact also provide commercial haptic interface products that allow forces to be applied to catheters and guidewires.

### 3 Materials and Methods

This section starts with a description of the components used by the simulation platform (see the subsection on ‘System description’). Next the pre-processing of the medical scanner data to create the patient specific anatomical models is described (see the subsection on ‘Data acquisition and visualization’). In the subsection on ‘Haptic rendering’, our volume haptic model for needle insertion is presented. Finally, the subsection on ‘Reconstructed image rendering’ details our new algorithm to simulate the image output from the virtual ultrasound probe. Local research ethics committee, and research governance approvals, were obtained for the use of all patient imaging data in this study.

### 3.1 System description

To interact with the virtual environment, any appropriate haptic interface can be used. Currently two Phantom haptic interfaces from SensAble Technologies have been selected. Devices such as the Phantom Omni (see Figure 3) or the Phantom Desktop both enable the trainee to feel the resistance of the tissue on the needle and the resistance of the skin on the image probe. The Phantom Desktop can provide higher fidelity, stronger forces and lower friction than the more cost-effective Phantom Omni. Despite this, Radiologists who tested the simulator confirmed that the force feedback from the Omni was close to the real sensations and the more expensive Phantom Desktop is not essential. To mimic the real experience as closely as possible the stylus on an Omni can also be replaced with a physical mock up of a real ultrasound transducer [16]. Right-handed radiologists usually prefer to manipulate the needle with their right hand whereas left-handed radiologists would prefer to use their left hand. The simulator therefore also allows the trainee to swap the virtual needle and the virtual image probe as desired.

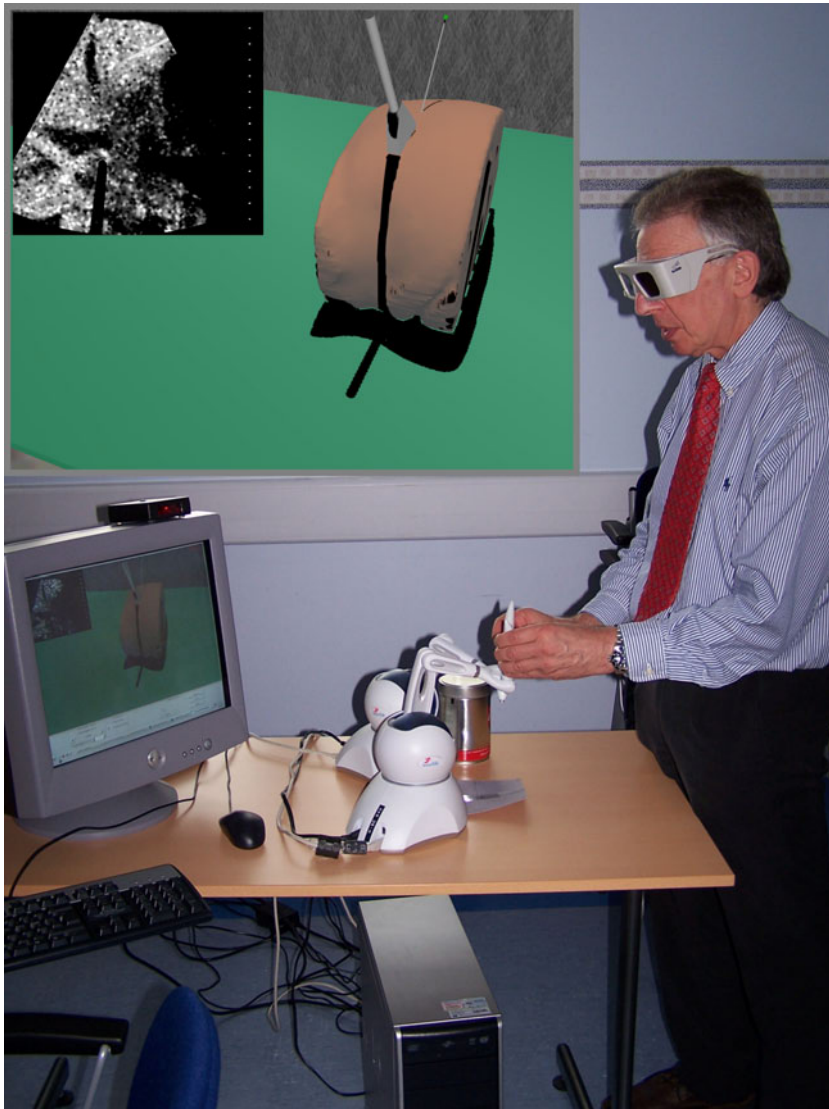


*Figure 3:* The simulator platform in use. The insert shows what the user will see on screen. Here, stereoscopy is enabled to improve positioning of the needle and probe at the skin entry site. Shadows are also rendered.

To further improve immersion, the virtual environment can be displayed in stereoscopy, e.g. using CrystalEyes shutter glasses and an infrared emitter from StereoGraphics Corporation. The effect for the trainee is that the 3D anatomy models appear to float in front of the screen, and can be presented as if the trainee is actually standing alongside the patient. The development computer used is a powerful dual 2 GHz Intel-Xeon processor with 2 GB of main memory and a NVIDIA Quadro FX 1000 graphics card. Nevertheless, the simulation has also been successfully tested on a standard PC with an AMD-Athlon XP 2000+ processor and 1.5 GB of main memory and an ATI Radeon 9600 PRO graphics card. Indeed, 3D textures, multi-texturing, framebuffer objects (FBOs) and vertex and fragment programs are nowadays commonly supported in hardware by modern graphics cards.

## 3.2 Data acquisition and visualization

Although the goal of this project is to deliver a training tool for freehand ultrasound guided needle puncture, 3D ultrasound (US) data sets are not used in our implementation. Such data is not readily available in the hospital for all patients and CT remains the most commonly used modality for 3D data sets. A smooth polygonal surface representing the relevant part of the patient's body must be generated to mimic the behaviour of an image probe moving over the skin of the patient. The extraction of the skin surface from 3D US is a challenging problem, however, due to the noise and artefacts in the data. Moreover, our volume haptic model for needle insertion (see the subsection on 'Needle haptic rendering') relies on the voxel intensities when calculating resistance according to the tissue properties at the needle tip. The range of intensities from 3D US has proved unsuitable for this approach.

CT has proven to be a valid data source for our simulator. It is a non-destructive imaging technique commonly used in hospitals for diagnosis, and provides reconstructed volume data of internal structures of the human body. The resulting stack of 2D trans-axial slices defines a voxel data set. Medical scanners deliver this data using the Digital Imaging and Communications in Medicine (DICOM) standard. Patient specific CT data is therefore theoretically easy to obtain, though first requires careful attention to research ethics and research governance requirements. A pre-processing step is applied to segment models of the patient's skin surface, skeleton structure and other relevant anatomy using the well known marching cubes algorithm [21]. This represents the surface as a triangular mesh and can be exported into a suitable file format, for example, using the standard Virtual Reality Modelling Language (VRML). Transparency can also be used when rendering these anatomy models, which is useful for the trainee in the early learning stages to help understand the relationship of needle, patient and image from the transducer. However, at the end of training the skin surface will remain fully opaque.

An alternative method would be to represent the virtual patient by volume rendering the CT data set. However, this technique proved to be too slow for use in our simulator, even when using a powerful graphics card. Volume rendering also still requires pre-segmentation of the internal organs of interest.

## 3.3 Haptic rendering

Two haptic devices are attached to the computer. The first acts like a virtual image probe, e.g. an ultrasound transducer. As the trainee moves the probe over the surface of the virtual body, he/she is provided with appropriate force feedback so that contact between the probe and the skin can be maintained. The image plane corresponding to the position and orientation of the probe is computed simultaneously (see the subsection on 'Reconstructed image rendering') and displayed in realtime in a sub-window of the virtual environment (see Figure 3). The second haptic device behaves like a needle and can puncture through the virtual skin and tissue layers. If the needle intersects the image plane of the probe, then the trainee will see the needle on the reconstructed image.

To achieve acceptable tactile and force feedback perception during the simulation, it is widely accepted that the minimal haptic refresh rate must be 1 kHz. However, refresh rates suitable

for real-time graphics must be at least 10-30 Hz. Thus the haptics and graphics renderings are normally disassociated. On mono-processor computers, this can be achieved by using a special timer for haptics. On computers with several processors, in order to take advantage of the parallel architecture, this can be achieved by making use of multiple threads. In the latter case, care must be given to manage concurrent access to the data written by the haptics thread and read by the graphics thread, and *vice versa*.

The subsections below describe the haptic rendering algorithms developed to mimic an ultrasound probe and a needle respectively. The first one is a hybrid model which combines i) the proxy-based algorithm on the polygon mesh of the skin surface and ii) a haptic volume rendering algorithm using the CT dataset to include hard structures such as bony landmarks. The second one can be subdivided into two separate models: before penetrating the skin, the needle can be used to explore its surface; after entering the skin, the needle can be used to penetrate internal tissues. Care is also taken to prevent the needle penetrating bones, to match with real world conditions.

### 3.3.1 Ultrasound probe haptic rendering

A proxy-based algorithm [30] is commonly accepted for the haptic rendering of surfaces. The haptic device interacts with the surface of a 3D object, usually represented as a triangular polygon mesh. In the proxy-based algorithm, a small sphere, the virtual proxy, represents the desired position of the device. Although the device can penetrate into the object with which it is interacting, the proxy always remains outside of its surface. At each iteration of the algorithm, the proxy is moved in order to minimise its distance to the actual device, in other words the proxy is the point on the surface that is the closest to the actual device position. Then, the surface will constrain the haptic device to reach the proxy using a force proportional to the distance ( $\Delta x$ ) between the proxy and the actual device, the force feedback is then similar to a spring effect using the Hooke's Law:  $\mathbf{F} = -k\Delta x$ . By manipulating the constant  $k$ , the stiffness of the object can be modified.

When scanning the surface of the virtual patient, the above model does not natively take into account any internal structures, particularly hard structures such as bony landmarks. However, interventional radiologists locate the site for probe placement, and needle access using palpation of bone and soft tissue landmarks. There is therefore a requirement to include a similar feature in the simulator. It is not at present possible to reproduce the sensation of palpation of the virtual patient using the operator's actual hand. As an alternative, the trainee is able to feel bones through the resistance of the 'tissues' beneath the probe mockup. Under these conditions, the force feedback obtained should constrain the device to remain outside the bone. Here, using the voxel values in the CT volume dataset, we propose a hybrid model based on the Chai3D [6] implementation of the proxy-based algorithm. As Figure 4 illustrates, if any hard structure is detected along the straight line between the proxy and the actual position of the device, i.e. any voxel intensity between the proxy and the position of the device is higher than a given threshold, then the proxy is moved to the entry point of the straight line from the proxy to the device position into the detected voxel, i.e. the surface of the touched bone. In this case, the stiffness will be increased to simulate a hard object. If no hard structure is detected, then the "classic" proxy-based algorithm is used as normally. Testing the voxel intensities between the two end points of a line segment can be efficiently implemented using ray tracing through voxel data. In this case, voxels are modelled using axis-aligned parallelepiped boxes made of three pairs of parallel planes [37]. To prevent large force discontinuities between two successive iterations when the device is being moved into hard structures, force smoothing is used [19]. Note also that this model does not introduce any instability or shaking of the device because the resulting force is always parallel to the force that would have been given by the "classic" proxy-based algorithm.

### 3.3.2 Needle haptic rendering

The force feedback delivered in virtual environment (VE) simulator models is generally an approximation to a real procedure, as assessed by experts. In virtual environment training systems,

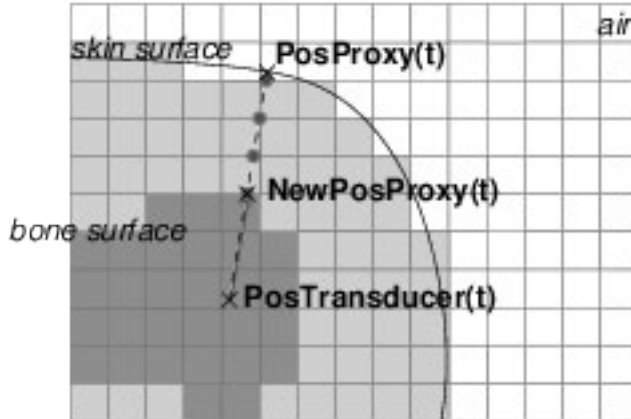


**Figure 4:** Force feedback when the transducer is in contact with bones (with **PosProxy(t)** the proxy position used normally in the “classic” proxy-based algorithm - **NewPosProxy(t)** the position at the surface of bones of the modified proxy - **PosTransducer(t)** the device position - all necessary intersections between voxels and a ray from **PosProxy** to **PosTransducer** in white dots).

haptics based on real procedural forces should allow a more authentic simulation of the subtle cues perceived when carrying out an interventional procedure in real world conditions [15]. In evaluating needle puncture procedures, for example, *in vitro* studies are essential for detailed understanding of the physical components and effects of overall summated forces. Prior work includes needle insertion forces in porcine and bovine tissues [3, 32]. Our clinical collaborators are collecting such experimental data [14]. Nevertheless, due to the different physical properties of living tissues, *in vitro* data require verification by *in vivo* measurements [27]. Until recently there were few devices available for measurement of instrument forces *in vivo* in humans, unobtrusively: flexible capacitance pads [28] present a novel opportunity to collect these data *in vivo* and calibration *in vitro* has shown that the output is stable and reproducible [14]. Work has also been performed to estimate both the force required, and the soft tissue deformation during the insertion of a 17 gauge Tuohy needle into a phantom made of a polyvinyl chloride compound [9, 10].

Currently, there is still a shortage of experimental data on tissue resistance. Our clinical collaborators are collecting such force data from a tensile tester used *in vitro*. To date, resistance data of the kidney and the liver is available for punctures with different kind of needles. Only data for Chiba needle is of interest here as this is the needle that is often used for gaining access to the kidney, which is a typical example of the visceral interventional needle puncture procedures that we are simulating. Obviously, there is no skin or subcutaneous tissue in the measurements. Figure 5a shows the resistance force of a porcine kidney. A porcine kidney has been used because the porcine and human anatomies are relatively similar. A Chiba needle is mounted and driven into the tissue at a fixed velocity, 500 mm per minute. This is an approximation of the speed of needle insertion during interventional radiological procedures. The needle orientation was normal to the surface of the kidney. Ten punctures were repeated to obtain an average and a range of forces involved. As it can be seen on Figure 5a, there is an initial displacement, approximately 10 mm, before the penetration of the kidney. Note that this initial displacement is important because in a live case the needle will at first push the kidney away, then a rebound into the force can be observed. It is followed by a plateau phase, although the force slightly increases with the depth of penetration. The black line in Figure 5a is an approximation of the slope of this plateau. The parameters of its equation are estimated using a non-linear least-squares algorithm [1]. As illustrated by the green curve in Figure 5a, it is also possible to fit an analytic model directly to the measurements. In our case, this model corresponds to a sum of eight Gaussian functions whose parameters are estimated once again using a non-linear least-squares algorithm.

Similar data is also available for bovine livers (see Figure 5b). There is also an initial dis-

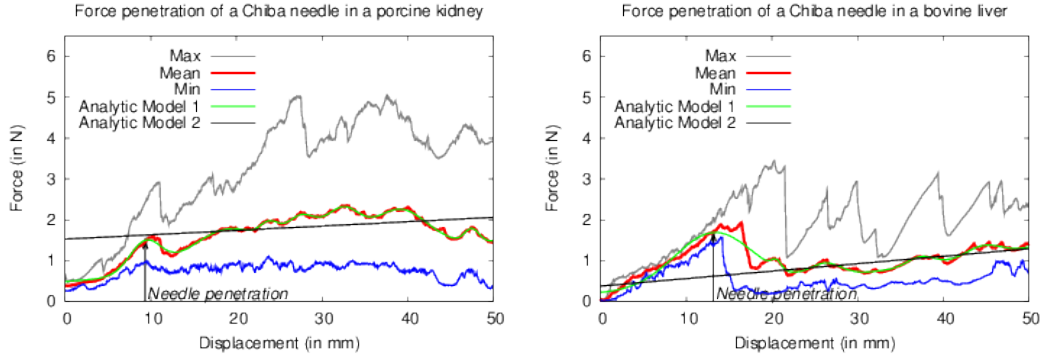


**Figure 5:** Force penetration of a Chiba needle from a tensile tester used *in vitro* (needle velocity = 500 mm.min<sup>-1</sup>), a) in a porcine kidney on the left-hand side, and b) in an bovine liver on the right-hand side.

placement before the penetration of the liver, followed by a rebound into the force, then a plateau phase, although the force slightly increases with the depth of penetration. Figure 5 shows that to insert the needle into the kidney, more resistance is applied on the needle than for the insertion into the liver.

The experimental data presented here cannot be used directly in the simulation as it does not provide a comprehensive description of tissue resistance. Nevertheless, the haptic model described below aims to reproduce the same trend as shown by the experimental data, i.e. higher force before the penetration of the tissue followed by a plateau phase. The slope of the plateau phase being relatively small, the depth of penetration is not taken into account. As shown in Figure 5, the average resistance force of the liver and kidney is lower than the maximum force that the Phantom Omni and the Phantom desktop can output, 3.3 N and 7.9 N respectively (see [31]). This is the same for the maximum force resistance of the bovine liver. The maximum resistance force of a porcine kidney is also lower than the maximum force that the Phantom Desktop can output, but significantly higher than the maximum force of the Phantom Omni. Similarly, the continuous exertable force that these devices can output, i.e. during 24 hours, is significantly lower than the tissue resistance (0.88 N in the case of the Phantom Omni, and 1.75 N for the Phantom Desktop). However, we are also investigating support for larger forces with devices that apply force directly to the point of contact through tension in cables (e.g. Mimic technologies Mantis).

As stated previously, we can distinguish two different usages of the needle. It can be used for exploring the skin surface before penetration, and it can also be used to penetrate internal tissues. In exploring the surface, normal practice is to first anaesthetise the skin with lignocaine, followed by a small skin incision to facilitate needle entry. The needle is then carefully placed into this skin ‘nick’, often by gently dragging the tip across the skin until it ‘drops’ into the skin incision. The needle can then be advanced to penetrate the tissues. During the penetration phase, different features have been identified: higher forces are generated at the interface between two different tissues, with a plateau phase. There is also a very high force with contact with bones. Indeed, the haptic rendering should prevent a needle from penetrating into bones. Our system uses two different haptic models to mimic the needle manipulation. Before penetrating the skin surface, the proxy-based algorithm can again be used, but with different friction parameters to mimic a needle moving over the skin surface. When the force applied by the needle at the insertion point exceeds a given threshold, the haptic rendering mode is switched to a secondary mode that allows the needle to penetrate internal tissues. This can be represented as:

$$\mathbf{F}(\mathbf{t}) = \mathbf{F}_1(\mathbf{t}) + \mathbf{F}_2(\mathbf{t}) + \mathbf{G} \quad (1)$$

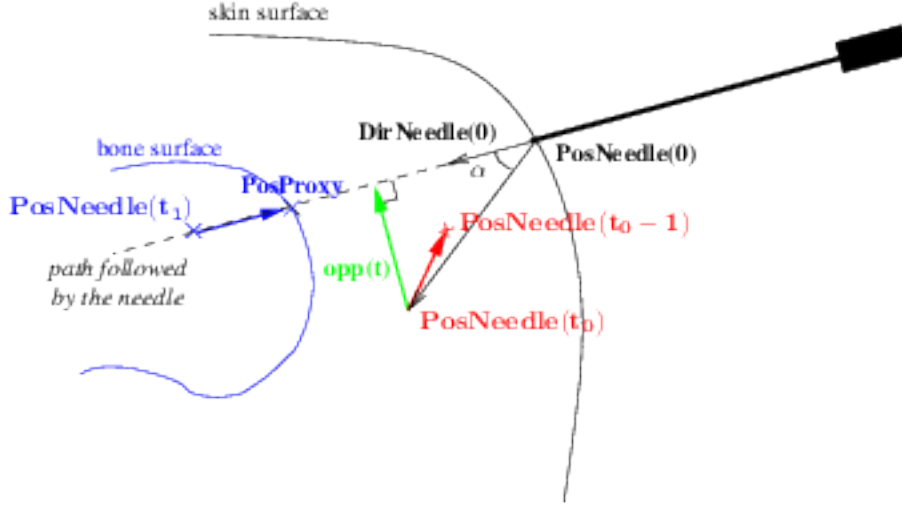


**Figure 6:** Forces in action during the insertion of the needle (with  $\mathbf{PosNeedle}(t)$  and  $\mathbf{DirNeedle}(t)$  as the needle position and direction at time  $t$  respectively,  $t$  is equal to 0 at the beginning of the insertion). In red would be reaction force to the soft-tissue's resistance at time  $t_0$ . In blue would be force constraining the needle to remain outside bones at time  $t_1$  ( $\mathbf{PosProxy}$  is the last position of the needle tip before contact with bones). In green would be force constraining the needle to follow a straight line.

where  $\mathbf{F}(t)$  is the reaction force returned to the haptic device at time  $t$  as illustrated by the coloured arrows in Figure 6 ( $t$  is equal to 0 at the beginning of the insertion).  $\mathbf{G}$  is a constant force correcting the effect due to gravity.  $\mathbf{F}_1(t)$  and  $\mathbf{F}_2(t)$  can be derived as follows:

- (i)  $\mathbf{F}_1(t)$  represents the reaction force to the tissue's resistance as the needle penetrates deeper. Three different sub-models are used to compute  $\mathbf{F}_1(t)$  depending whether: a) the needle is penetrating tissues, b) the needle is in contact with bone, or c) the needle is being pulled out.
- (a) Let  $\mathbf{PosNeedle}(t)$  be the vector defined by the needle position at time  $t$ . When the needle is pushed harder, the resistance of the tissue increases, i.e.  $|\mathbf{PosNeedle}(t-1) - \mathbf{PosNeedle}(t)|$  will be higher and so the trainee will feel more resistance. Let  $\mathbf{F}_{1a}(t)$  be the reaction force in a model based on Hooke's law where the reaction effect will be proportional to the depth of penetration of the needle between time  $t-1$  and time  $t$  (see red arrow in Figure 6):

$$\mathbf{F}_{1a}(t) = K_1 * (\mathbf{PosNeedle}(t-1) - \mathbf{PosNeedle}(t)) \quad (2)$$

where  $K_1$  is a constant that relates to the tissue properties.

However, using such a model to calculate the force, the trainee may feel the needle vibrate. To improve stability, the reaction force is averaged using a digital filter over the last  $m$  iterations, giving:

$$\mathbf{F}_1(t) = \frac{1}{m} * \sum_{i=t-m}^t \mathbf{SubForce}(i) \quad (3)$$

where

$$\mathbf{SubForce}(i) = K_1 * (\mathbf{PosNeedle}(i-1) - \mathbf{PosNeedle}(i)) \quad (4)$$

To take into account the tissue properties at the tip of the needle,  $K_1$  is replaced in the final model (Eq. 5 & 6) by  $LUT(VI(\mathbf{PosNeedle}(i)))$ , where  $VI(\mathbf{PosNeedle}(i))$  is the

voxel intensity at the position of the needle tip in the CT dataset. Tissue properties are thus extracted from a look up table (LUT). To give smoothed variations between the ranges of voxel intensities that characterize tissues, the LUT is represented as a B-spline. Its x-axis is the voxel intensity in standard Hounsfield units, and its y-axis is the resistance coefficient for the given voxel intensity. More resistance is given to hard structures, such as bone, and less resistance to soft tissues. This profile is then manually tuned using experimental force measurements acquired *in vitro* or during procedures on patients in the IR operating theatre [14], e.g. more resistance can be given to the range of voxels corresponding to the kidney than to the range of voxels that corresponds to the liver. Then, the reaction force of the needle to tissue resistance in Eq. 3 can be represented as:

$$\mathbf{SubForce}(\mathbf{i}) = LUT(VI(\mathbf{PosNeedle}(\mathbf{i}))) * (\mathbf{PosNeedle}(\mathbf{i} - \mathbf{1}) - \mathbf{PosNeedle}(\mathbf{i})) \quad (5)$$

When the needle passes from one tissue type to another, a higher force can be observed [14]. In the final model, this is taken into account by multiplying  $LUT(VI(\mathbf{PosNeedle}(\mathbf{i})))$  by a constant value,  $K_{edge}$ , when the tip of the needle is positioned at the interface between two tissue types. If the gradient magnitude at this position in the volume dataset is higher than a given threshold, then the needle is located at the interface between the tissues, and the force feedback will be higher. In this case, Eq. 5 becomes:

$$\mathbf{SubForce}(\mathbf{i}) = K_{edge} * LUT(VI(\mathbf{PosNeedle}(\mathbf{i}))) * (\mathbf{PosNeedle}(\mathbf{i} - \mathbf{1}) - \mathbf{PosNeedle}(\mathbf{i})) \quad (6)$$

where  $K_{edge} > 1$ .

- (b) The described model (Eq 3, 5 & 6) gives acceptable results for simulating tissue penetration. In the case of tissue that cannot be penetrated, e.g. bones, the model is not well adapted. Indeed, in such a case the force rendering needed to prevent penetration must be much higher, and the model becomes unstable. To prevent this, when  $VI(\mathbf{PosNeedle}(\mathbf{i}))$  corresponds to bones,  $\mathbf{F}_1(\mathbf{t})$  is changed to a sub-model similar to the proxy-based algorithm [30]. In our new sub-model, the virtual proxy represents the position of the device when it enters into the bone (see blue arrow in Figure 6). The proxy always remains outside the bone surface whereas the device can slightly penetrate into the bone. The haptic device will be constrained to reach the proxy outside the bone, using the following sub-model in Eq. 3:

$$\mathbf{SubForce}(\mathbf{i}) = K_{bone} * (\mathbf{PosProxy} - \mathbf{PosNeedle}(\mathbf{i})) \quad (7)$$

where  $\mathbf{PosProxy}$  is the position of the needle at the contact with bones.

- (c) When the needle is being removed, the force applied to the needle is relatively constant. Then, if the dot product between  $(\mathbf{PosNeedle}(\mathbf{t}) - \mathbf{PosNeedle}(\mathbf{t} - \mathbf{1}))$  and  $\mathbf{DirNeedle}(\mathbf{0})$  is negative,  $LUT(VI(\mathbf{PosNeedle}(\mathbf{i})))$  is replaced by a constant value in Eq. 5.
- (ii) In the real procedure, it is difficult to move the needle off its initial trajectory. In the simulation, once the needle is within the body, it is therefore constrained to follow the path defined by its orientation at the entry point (see green arrow in Figure 6).  $\mathbf{F}_2(\mathbf{t})$  corresponds to the required constraining force, which is perpendicular to the needle path:

$$\mathbf{F}_2(\mathbf{t}) = K_2(|\mathbf{F}_c(\mathbf{t})|) * \mathbf{F}_c(\mathbf{t}) \quad (8)$$

where

$$\mathbf{F}_c(\mathbf{t}) = \frac{K_3}{n} * \sum_{j=t-n}^t \mathbf{opp}(\mathbf{j})$$

$$K_2(x) = (1 - \text{gauss}(x)) \quad \forall x, K_2(x) \in [0, 1]$$

$K_3$  is a constant set empirically in accordance to the desired effect and  $\text{gauss}(x)$  is a Gaussian function.  $\mathbf{opp}(\mathbf{t})$  can be calculated using basic trigonometric functions on  $\mathbf{DirNeedle}(\mathbf{0})$ ,  $\mathbf{PosNeedle}(\mathbf{0})$  and  $\mathbf{DirNeedle}(\mathbf{t})$ , which are known values. Once again, to improve stability, the constraining force is averaged over the last  $n$  iterations. To avoid the needle vibrating if it is slightly perturbed from its constrained trajectory, i.e. when the distance  $|\mathbf{F}_c(\mathbf{t})|$  is negligible,  $K_2(x)$  is used to smoothly clamp the constraining force to null.

The Phantom devices used in the simulation provide 6 degrees of freedom (DOF) in motion, and 3 DOF in force feedback, so the trainee can move the stylus of the haptic device in all directions and orientations (pitch, roll and yaw), but the force feedback is only applied on the end point of the stylus. A detrimental effect of this is that during the puncture the trainee is able to rotate the pitch and yaw of the needle because the device is not designed to provide any force feedback on rotations. Devices with 6 DOF in force feedback do not have this problem but their significantly higher cost prohibits their use in cost effective medical simulators. To address this drawback, our clinical collaborators recommended not tracking the orientation of the device stylus during the puncture stage. Nevertheless, in actual procedures, after penetrating the skin and whilst the needle is still in superficial tissues, the clinician may have to change the needle angle to successfully reach the target. Consequently the needle orientation is not tracked during the puncture stage unless the needle tip remains 2 cm below the skin surface. This tradeoff does have some impact on the simulator fidelity, however, our clinical collaborators have found the 3 DOF Phantom to be acceptable.

### 3.4 Reconstructed image rendering

As the trainee moves the image probe over the skin of the virtual patient, an image corresponding to the position and orientation of the image plane is computed and displayed in realtime (see Figure 3). The goal is to display the image using a variety of formats, including ultrasound, fluoroscopy and CT. This Section describes how to approximate ultrasound images - a description of our fluoroscopy simulator is available in [36]. For US images, the first step is to use a 2D multiplanar reconstruction (MPR) image, i.e. an oblique image computed from the original set of parallel CT slices. The MPR image can be directly computed by “reformatting” the input CT data, but without hardware support this technique has proved to be too slow for updating images in realtime with a good resolution. During the procedure the operator/trainee uses the displayed image to guide the needle puncture, and so the needle must appear on the image as it is being inserted. This can be achieved by assigning to those voxels penetrated by the needle a high value corresponding to the metallic material of the needle shaft, which both highly attenuates x-rays, and reflects ultrasound. A flexible scheme for generating the images with full hardware acceleration is explained below, and its rendering pipeline is illustrated in Figure 7. It is implemented using OpenGL, a cross-platform standard 3D graphics API (Application Programming Interface).

Modern graphics cards support 3D texturing, which can be exploited to provide hardware acceleration for computing the MPR image. Nevertheless, it is not possible to update the content of the 3D texture in realtime to change the voxel intensities at the needle position because of the overhead involved in transferring the recalculated data from main memory to the graphics card. An important new development in graphics programming, however, is the use of high-level programming languages to take control over critical stages of the graphics rendering pipeline. Using the new OpenGL shading language (GLSL), it is now possible to avoid the limitations of the fixed graphics rendering pipeline and to take advantage of programmable graphics hardware. Using GLSL, it becomes possible to detect if the texture coordinates corresponding to each pixel of the MPR image, computed from the 3D texture, are either being penetrated by the needle or not. Thus, the straightforward algorithm using trigonometric identities described previously in [35] can also be implemented using GLSL to use hardware acceleration to detect whether texture coordinates corresponding to the voxel  $V$  in the original CT dataset should be marked as a needle

voxel (see [35] for details). In such a case, the pixel in the MPR image is directly set to a high value instead of fetching the original colour at the given texture coordinates (see Figure 7a).

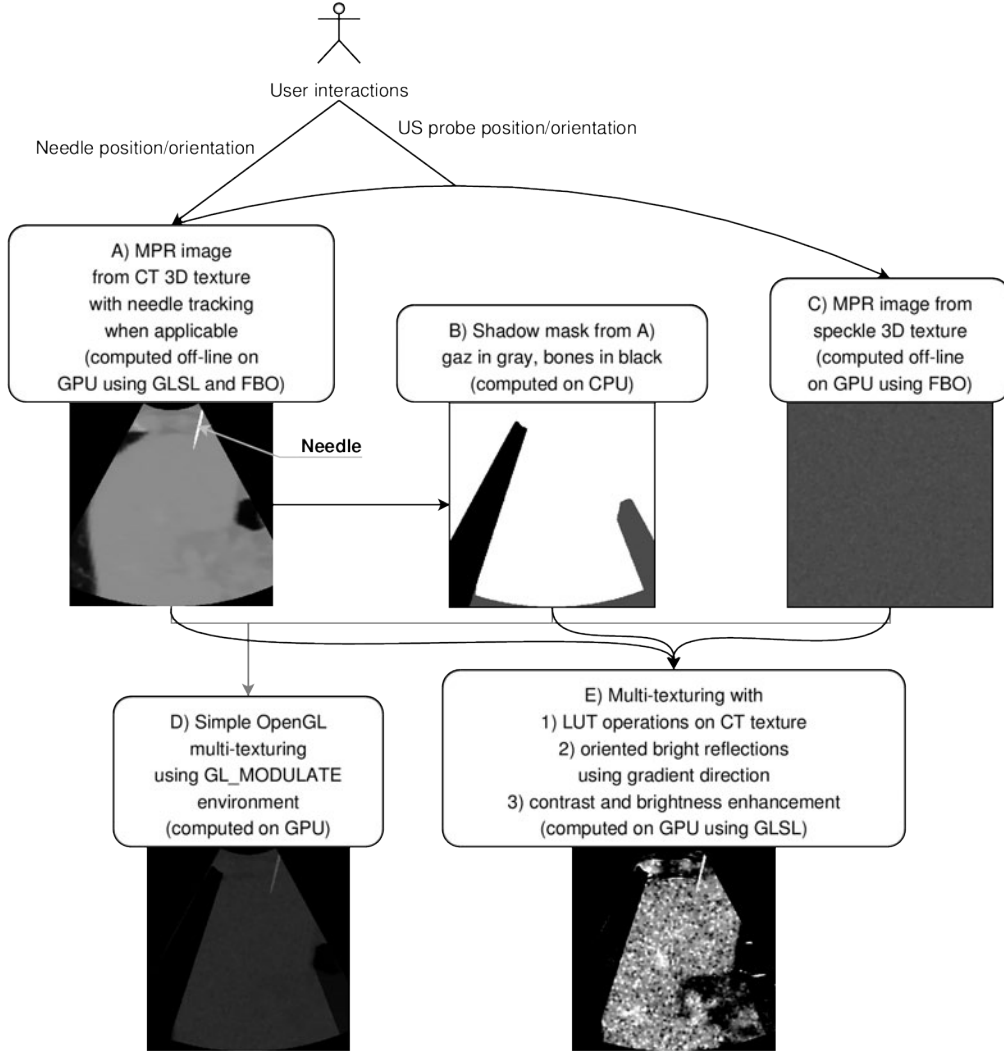


**Figure 7:** Graphics rendering pipeline: A) MPR image; B) gas & bone shadow-mask; C) image of noise; D) OpenGL multi-texturing rendering combining the three previous images; E) final ultrasound-like image.

In ultrasound imaging, hard structures such as bones totally reflect the ultrasound signal. On corresponding images, pixels located behind such structures are therefore in “shadow”. Similarly, pixels located behind gas also appear darker due to sound reflection at the tissue/gas interface (acoustic shadowing). This effect can be simulated by post-processing the MPR image to compute a shadow mask (see Figure 7b). Every pixel of the mask is initialized to the value “1”. To compute the mask, every column is processed as follows: every pixel in the MPR image behind a pixel whose intensity is higher or lower than given thresholds corresponding to bones or gas is set to a smaller value into the mask. Such computation cannot be performed efficiently using GLSL because each pixel is treated independently. Consequently, this task has to be performed on the CPU. The MPR image is then computed efficiently using the offline rendering capability of the graphics card offered by the framebuffer object (FBO) available as a relatively new extension of the OpenGL API [26].

As it can be seen in Figure 2, high-frequency noise is observed in real ultrasound images. In

our simulation, the noise is represented using a stack of “noisy” 2D slices. This data is loaded into the memory of the graphics card as a 3D texture. An MPR image of noise depending on the probe position and orientation is then computed using hardware acceleration (see Figure 7c).

Bright reflections may also occur in US images at interfaces with bone or gas, but also with fat/tissue and other interfaces. This effect can be produced in the final image by detecting and enhancing horizontal edges in the MPR image. It can be achieved by post-processing the MPR image using a Sobel filter to compute the gradient direction (see Figure 7e). Reflections will occur when the gradient direction along the vertical axis of the image is above a given threshold.

In the final rendering stage, all generated images (the MPR image, the shadow mask and the noise slice) are used as 2D textures and blended using multi-texturing. This can be achieved using the fixed rendering pipeline of the graphics card, multiplying the textures together pixel by pixel, as illustrated by Figure 7d. However, the fixed rendering pipeline does not provide sufficient flexibility and performance to transform the pixels of the MPR image into an US appearance in realtime via a lookup table (LUT). It also prevents the computation of reflections during the rendering stage. Our solution is to efficiently generate these effects (LUT operations, multi-texturing, reflections at interfaces, and also interactive contrast/brightness enhancement) in a single rendering-pass using GLSL (see Figure 7e).

## 4 Results

An integrated simulator for image guided needle puncture has been produced. It has been tested on a variety of platforms from a standard desktop PC with an ATI Radeon 9600 PRO to a state-of-the-art workstation with the far more powerful NVIDIA Quadro FX 3400 graphics card, and provides interactive performance in all cases ( $\sim 24$  frames per second [FPS] on a standard PC, and  $\sim 60$  FPS on the workstation). A goal has been to provide a cost effective solution. Inexpensive components are used wherever possible, and the configuration used can be tailored to match a variety of budgets.

The simulator has been developed in close collaboration with practicing interventional radiologists. In particular, we have made use of IR task analysis studies that have been carried out by our collaborators [18]. For feed back on each stage of development, informal face and content validation studies were conducted by medical collaborators during informal visits to ensure that the fidelity of the simulator attains an acceptable level. In further, objective evaluations, questionnaires were developed to evaluate the features and the performances of the simulator. These were distributed to trainees and experts at three different workshops. Two of these workshops, were at a large teaching hospital, and were held at intervals of one year. At both of these the simulator was exposed to a group of inexperienced IR trainees. At a third workshop, experienced IR practitioners from Europe and the US were allowed to experience the simulator in a large conference setting. The data obtained from the questionnaires given to trainees during the two workshops at the teaching hospital is shown in Tables 2 and 3 respectively. Many suggestions for improvements were collected and subsequently integrated into the simulator. One issue identified was the placement of the haptic interfaces in relation to the virtual patient. Placing the Phantoms side by side in front of the computer monitor is not an appropriate mapping to real world conditions. The Phantoms both needed to be turned through 45 degrees to give a more natural interface and to avoid potential collisions between the haptic arms (see Figure 3), and the software was therefore updated to allow for this. Another issue was related to the use of stereoscopy. The version of the simulator used at the first workshop at the teaching hospital was an early version of the simulator that made use of an immersive virtual environment with stereoscopy [35]. At the second workshop, the simulator described in this paper was used on a laptop without stereoscopy. Placing the virtual probe and needle at the skin entry site then became more difficult to achieve. Therefore, to further improve the depth perception, we are now investigating the use of shadowing of the needle and ultrasound probe on the patient’s skin (see Figure 3). However, when the needle is being inserted through the tissues, the visual cue is exclusively taken from the 2D image being displayed. The original simulator was designed so that the whole procedure is carried out

|    |   |                            |                          |                   |                       |                         |                       |
|----|---|----------------------------|--------------------------|-------------------|-----------------------|-------------------------|-----------------------|
| 1) | <b>The visual rendering is good enough for training</b>   |                            |                          |                   |                       |                         |                       |
|    | <i>Strongly disagree</i>  | <i>Moderately disagree</i> | <i>Slightly disagree</i> | <i>Don't know</i> | <i>Slightly agree</i> | <i>Moderately agree</i> | <i>Strongly agree</i> |
|    | 0%  | 10%                        | 0%                       | 10%               | 15%                   | 50%                     | 15%                   |
| 2) | <b>It is fundamental to hold two force-feedback devices at the same time (one for the needle, one for the ultrasound probe)</b> |                            |                          |                   |                       |                         |                       |
|    | <i>Strongly disagree</i>  | <i>Moderately disagree</i> | <i>Slightly disagree</i> | <i>Don't know</i> | <i>Slightly agree</i> | <i>Moderately agree</i> | <i>Strongly agree</i> |
|    | 0%  | 0%                         | 0%                       | 10%               | 15%                   | 25%                     | 50%                   |
| 3) | <b>During the scanning of the body, the force feedback is realistic enough for a training tool</b>                              |                            |                          |                   |                       |                         |                       |
|    | <i>Strongly disagree</i>  | <i>Moderately disagree</i> | <i>Slightly disagree</i> | <i>Don't know</i> | <i>Slightly agree</i> | <i>Moderately agree</i> | <i>Strongly agree</i> |
|    | 0%  | 0%                         | 10%                      | 5%                | 25%                   | 40%                     | 20%                   |
| 4) | <b>During the puncture, the force feedback is realistic enough for a training tool</b>  |                            |                          |                   |                       |                         |                       |
|    | <i>Strongly disagree</i>  | <i>Moderately disagree</i> | <i>Slightly disagree</i> | <i>Don't know</i> | <i>Slightly agree</i> | <i>Moderately agree</i> | <i>Strongly agree</i> |
|    | 0%  | 5%                         | 25%                      | 5%                | 35%                   | 15%                     | 15%                   |
| 5) | <b>When the simulator would be fully developed, you think it would be worth to initially train on the simulator</b>             |                            |                          |                   |                       |                         |                       |
|    | <i>Strongly disagree</i>  | <i>Moderately disagree</i> | <i>Slightly disagree</i> | <i>Don't know</i> | <i>Slightly agree</i> | <i>Moderately agree</i> | <i>Strongly agree</i> |
|    | 0%  | 0%                         | 5%                       | 0%                | 5%                    | 35%                     | 55%                   |

**Table 2:** Data obtained from the questionnaires given to twenty inexperienced trainees during the first workshop at the teaching hospital, using the early version of the simulator described in [35]. Trainees were asked to fill out this questionnaire by circling the alternative that they agree most. The number of answers for each question is given in percentage.

in stereo. This has now been made optional as it is not needed for the second stage of the needle puncture procedure, and the requirement to wear stereo glasses can be removed. Through such enhancements, the simulator has reached a point where it is now suitable for a concurrent validity test (where novice and expert performance will be compared) and this is currently being planned. Indeed, our preliminary demonstrations during workshops amongst IR students or practitioners have demonstrated satisfactory performance in terms of haptic force feedback, system ergonomics, image clarity, and the usefulness of the simulator.

## 5 Conclusions and Future Work

Medical simulators have a significant role to play in providing a viable alternative to traditional apprenticeships in patients. However, the worldwide market for such simulators is still relatively small, and only a few companies are offering commercial products today. One factor has been the high cost associated with purchasing and maintaining the state-of-the-art equipment required. A goal of this project has been to demonstrate that off the shelf components can also be utilised to provide a cost effective simulator that still has all of the required functionality. Validation of the simulator is however critical to its uptake in a training curriculum and a project such as this cannot be undertaken without close co-operation with the domain experts. Hence task analysis and content validation have been important steps, and the results obtained are providing input to initiatives within the interventional radiology community to establish standards for metrics that are to be used to assess trainee performance. For example, members of this project are involved in a joint medical simulation task force formed by the Cardiovascular and Interventional Radiological Society of Europe (CIRSE), the Society of Interventional Radiology (SIR) and the Radiological

| Questions |  | Average answer | Standard deviation |
|-----------|--|----------------|--------------------|
| 1.        | <b>Age:</b>  | 30.42          | 2.59               |
| 2.        | <b>Number of years in radiology:</b>   | 1.68           | 1.11               |
| 3.        | <b>How confident do you feel when performing imaging guided needle puncture procedures?</b><br>(1=no confidence; 10=full confidence)   | 4.32           | 1.53               |
| 4a.       | <b>How many IR procedure performed this last 3 months (in total)?</b>  | 8              | 6.97               |
| 4b.       | <b>independently?</b>  | 2              | 4.26               |
| 5.        | <b>How similar did you find the procedure on the simulator model to the same kind of procedure in patient?</b> (1=very different, 2=fairly different, 3=neutral, 4=fairly similar, 5=very similar) | 2.26           | 1.05               |
| 6.        | <b>How much do you agree with the following statements:</b><br>(1=strongly disagree, 2=somewhat disagree, 3=acceptable, 4=somewhat agree, 5=strongly agree)  |                |                    |
|           | <b>Simulation of the patient environment:</b>  |                |                    |
| i)        | CT visual elements were of high quality  | 3.89           | 0.94               |
| ii)       | Tactile (touch) elements were accurate   | 2.58           | 0.69               |
|           | <b>Simulation of the needle insertion procedure:</b>   |                |                    |
| iii)      | Needle insertion through skin is realistic   | 2.63           | 0.96               |
| iv)       | Needle insertion through tissues is realistic  | 2.84           | 0.83               |
|           | <b>General:</b>  |                |                    |
| v)        | The level of difficulty of the cases were appropriate  | 3.22           | 0.88               |
| vi)       | The cases covered situations encountered in my practice  | 3.28           | 1.02               |
| vii)      | The cases were a suitable challenge for my skills  | 3.33           | 0.97               |
| viii)     | The simulator reflected a high level of realism  | 2.61           | 0.92               |

**Table 3:** Data obtained from the questionnaires given to nineteen inexperienced trainees during the second workshop at the teaching hospital, using the version of the simulator described in this paper, and running on a laptop without stereoscopy capability. Trainees were asked to fill out this questionnaire by circling the alternative that they agree most.

Society of North America (RSNA). These bodies recognise the current shortfall in evidence for the effectiveness of existing IR vascular simulators, and are consequently setting out joint recommendations on the development and use of medical simulation to train and assess IR [13]. They have recently produced a strategy for its implementation into IR training curricula [2].

We have presented one of the first simulators to provide training for the commonly performed procedure of image guided needle puncture. The proxy-based haptic rendering method has been extended to use volumetric data so that the trainee can feel underlying structures, such as ribs, whilst scanning the surface of the body with the ultrasound transducer. An effective haptic model has been implemented that can be modulated by using actual force measurements. A method of approximating ultrasound-like images is also described. Future work to improve the functionality is planned. Tissue deformation, such as between the ultrasound transducer and the skin surface or between the needle and internal tissues, also needs to be improved. Warmth to touch, movement both of the patient and of internal structures (bowel and respiratory movement and pulsation of vessels) and audio feedback to the trainee as a result of pain or discomfort will also need to be simulated.

Finally, comprehensive construct and concurrent validation, and skills transfer studies, form

a key part of future, proposed work. This will be conducted within IR curricula to evaluate the clinical effectiveness of the simulator to train visceral needle puncture procedures.

## References

- [1] R. Aster, B. Borchers, and C. H. Thurber. *Parameter Estimation and Inverse Problems*. Academic Press, 2004.
- [2] G. J. Becker, B. Connors, J. Cardella, J. R. Duncan, S. L. Dawson, D. A. Gould, C. Glaiberman, D. O. Kessel, W. E. Lewandowski, D. Sacks, M. Sapoval, M. Scerbo, A. A. Patel, and R. Phillips. SIR and CIRSE joint medical simulation task force strategic plan. Available at <[http://www.cirse.org/\\_files/contentmanagement/CIRSE\\_SIR\\_Joint\\_Strategy.pdf](http://www.cirse.org/_files/contentmanagement/CIRSE_SIR_Joint_Strategy.pdf)> (accessed 7<sup>th</sup> March 2007).
- [3] P. N. Brett, T. J. Parker, A. J. Harrison, T. A. Thomas, and A. Carr. Simulation of resistance forces acting on surgical needles. *Proceedings of the Institution of Mechanical Engineers. Part H, Journal of engineering in medicine*, 211(4):335–347, Sept. 1997.
- [4] J. A. Carrino and F. A. Jolesz. MRI-guided interventions. *Academic Radiology*, 12(9):1063–1064, Sept. 2005. DOI: 10.1016/j.acra.2005.06.008.
- [5] G. A. Chapman, D. Johnson, and A. R. Bodenham. Visualisation of needle position using ultrasonography. *Anaesthesia*, 61(2):148–158, 2006. DOI: 10.1111/j.1365-2044.2005.04475.x.
- [6] F. Conti, F. Barbagli, D. Morris, and C. Sewell. CHAI: An open-source library for the rapid development of haptic scenes. Demo paper presented at World Haptics Conference (WHC’05), Mar. 2005.
- [7] CRaIVE - Collaboration in Radiological Interventional Virtual Environments. Website. <<http://www.craive.org.uk/>> (accessed 7<sup>th</sup> March 2007).
- [8] S. L. Dawson, S. Cotin, D. Meglan, D. W. Shaffer, and M. A. Ferrell. Designing a computer-based simulator for interventional cardiology training. *Catheterization and Cardiovascular Interventions*, 51(4):522–527, Dec. 2000. DOI: 10.1002/1522-726X(200012)51:4<522::AID-CCD30>3.0.CO;2-7.
- [9] S. P. DiMaio and S. E. Salcudean. Needle insertion modelling for the interactive simulation of percutaneous procedures. In *MICCAI ’02: Proceedings of the 5th International Conference on Medical Image Computing and Computer-Assisted Intervention-Part II*, pages 253–260, 2002.
- [10] S. P. DiMaio and S. E. Salcudean. Interactive simulation of needle insertion models. *IEEE Transactions on biomedical engineering*, 52(7):1167–1179, July 2005. DOI: 10.1109/TBME.2005.847548.
- [11] C. Forest, O. Comas, C. Vaysière, L. Soler, and J. Marescaux. Ultrasound and needle insertion simulators built on real patient-based data. In *Proceedings of MMVR 15*, pages 136–139, 2007.
- [12] E. Gobbetti, M. Tuveri, G. Zanetti, and A. Zorcolo. Catheter insertion simulation with co-registered direct volume rendering and haptic feedback. In *Proceedings of MMVR 2000*, pages 96–98, Jan. 2000.
- [13] D. A. Gould, J. A. Reekers, D. O. Kessel, N. C. Chalmers, M. Sapoval, A. A. Patel, G. J. Becker, M. J. Lee, and L. Stockx. Simulation devices in interventional radiology: Caveat emptor. *CardioVascular and Interventional Radiology*, 29(1):4–6, Feb. 2006. DOI: 10.1007/s00270-005-0354-z.

- [14] A. E. Healey, J. C. Evans, M. G. Murphy, S. Powell, T. V. How, D. Groves, F. Hatfield, B. M. Diaz, and D. A. Gould. In vivo force during arterial interventional radiology needle puncture procedures. In *Proceedings of MMVR 13*, pages 178–184, 2005.
- [15] E. A. M. Heijnsdijk, A. Padeloup, A. J. van der Pijl, J. Dankelman, and D. J. Gouma. The influence of force feedback and visual feedback in grasping tissue laparoscopically. *Surgical Endoscopy*, 18(6):980–985, June 2004. DOI: 10.1007/s00464-003-9244-0.
- [16] A. Hostettler, C. Forest, A. Forgione, L. Soler, and J. Marescaux. A real-time ultrasonography simulator based on CT-scan images. In *Proceedings of MMVR 13*, pages 191–193, 2005.
- [17] S. Johnson. Biopsy ultrasound guided TA. Available at <<http://www.hpv.cs.bangor.ac.uk/CRAIVE/ultrasound%20guided%20biopsy%20task%20analysis.pdf>> (accessed 7<sup>th</sup> March 2007).
- [18] S. J. Johnson, A. E. Healey, J. C. Evans, M. G. Murphy, M. Crawshaw, and D. Gould. Physical and cognitive task analysis in interventional radiology. *Journal of Clinical Radiology*, 61(1):97–103, Jan. 2006. DOI: 10.1016/j.crad.2005.09.003.
- [19] S. D. Laycock and A. M. Day. A survey of haptic rendering techniques. *Computer Graphics Forum*, 2007. To be published.
- [20] Limbs & Things. Medical simulation models. Website: <<http://www.golimbs.com/products/products.php?sectid=67>> (accessed 7<sup>th</sup> March 2007).
- [21] W. E. Lorensen and H. E. Cline. Marching cubes: A high resolution 3D surface construction algorithm. In *Proceedings of SIGGRAPH'87*, pages 163–169, 1987. DOI: 10.1145/37401.37422.
- [22] T. A. Matalon and B. Silver. US guidance of interventional procedures. *Radiology*, 174(1):43–47, Jan. 1990.
- [23] J. Merald. Interventional imaging: a new speciality in between radiology and surgery. *Bulletin de l'Académie Nationale de Médecine*, 175(7):1079–1084, Oct. 1991.
- [24] R. Otto and P. Deyhle. Guided puncture under real-time sonographic control. *Radiology*, 134(3):784–785, Mar. 1980.
- [25] J. P. Pedersen. Percutaneous nephrostomy guided by ultrasound. *Journal of Urology*, 112(2):157–159, 1974.
- [26] E. Persson. Framebuffer objects. ATI Radeon SDK documentation paper's collection, ATI Technologies, Inc., 2005.
- [27] V. K. Peter, J. Ward, K. Sherman, R. Phillips, and D. Wills. Force torque measurements during a routine knee arthroscopy: *in vivo* study. In *EFORT 6<sup>th</sup> Congress*, June 2003.
- [28] Pressure Profile Systems, Inc. Website. <<http://www.pressureprofile.com/>> (accessed 7<sup>th</sup> March 2007).
- [29] M. Raspolti, C. A. Avizzano, G. Facenza, and M. Bergamasco. HERMES: an angioplasty surgery simulator. In *Proceedings of World Haptics Conference (WHC'05)*, pages 148–156, Mar. 2005. DOI: 10.1109/WHC.2005.73.
- [30] D. C. Ruspini, K. Kolarov, and O. Khatib. The haptic display of complex graphical environments. In *Proceedings of SIGGRAPH'97*, pages 345–352, 1997. DOI: 10.1145/258734.258878.
- [31] SensAble Technologies, Inc. Website. <<http://www.sensable.com/>> (accessed 7<sup>th</sup> March 2007).

- [32] C. Simone and A. Okamura. Modeling of needle insertion forces for robot-assisted percutaneous therapy. In *Proceedings of the 2002 IEEE International Conference on Robotics and Automation (ICRA '02)*, pages 2085–2091, May 2002.
- [33] M. Sklair-Levy, A. Polliack, D. Shaham, Y. H. Applbaum, S. Gillis, D. Ben-Yehuda, Y. Sherman, and E. Libson. CT-guided core-needle biopsy in the diagnosis of mediastinal lymphoma. *European Radiology*, 10(5):714–718, Apr. 2000. DOI: 10.1007/s003300050991.
- [34] F. P. Vidal, F. Bello, K. W. Brodli, N. W. John, D. Gould, R. Phillips, and N. J. Avis. Principles and applications of computer graphics in medicine. *Computer Graphics Forum*, 25(1):113–137, Mar. 2006. DOI: 10.1111/j.1467-8659.2006.00822.x.
- [35] F. P. Vidal, N. Chalmers, D. A. Gould, A. E. Healey, and N. W. John. Developing a needle guidance virtual environment with patient-specific data and force feedback. In *Proceedings of CARS'05*, pages 418–423, May 2005. DOI: 10.1016/j.ics.2005.03.200.
- [36] F. P. Vidal, N. W. John, and R. M. Guillemot. Interactive physically-based x-ray simulation: CPU or GPU? In *Proceedings of MMVR 15*, pages 479–481, 2007.
- [37] A. Watt. *3D Computer Graphics*, chapter 1.4.4: Intersection - ray-box, pages 21–22. Addison-Wesley, 3<sup>rd</sup> edition, 2000.
- [38] Y. Zhu, D. Magee, R. Ratnalingam, and D. Kessel. A virtual ultrasound imaging system for the simulation of ultrasound-guided needle insertion procedures. In *Proc. Medical Image Understanding and Analysis (MIUA)*, volume 1, pages 61–65, July 2006.